

Reversible self-assembly of patchy particles into monodisperse clusters

Alex W. Wilber, Jonathan P. K. Doye,* Ard A. Louis*, Eva G. Noya, Mark A. Miller, and Pauline Wong

*Department of Chemistry, University of Cambridge,
Lensfield Road, Cambridge CB2 1EW, United Kingdom*

(Dated: July 15, 2019)

We systematically study the design of simple patchy sphere models that reversibly self-assemble into monodisperse clusters. The optimal patch width is a compromise between structural specificity (the patches must be narrow enough to energetically select the desired clusters) and kinetic accessibility (they must be sufficiently wide to avoid kinetic traps). Ordered clusters can form through a number of different dynamic pathways, including direct nucleation and indirect pathways through large disordered intermediates. For intermediate patch widths we find a reentrant liquid to gas transition upon lowering the temperature.

PACS numbers: 81.16.Dn, 47.57.-s

The remarkable ability of biological matter to robustly self-assemble into well defined composite objects excites the imagination, suggesting that these processes could perhaps be emulated through the judicious design of synthetic building blocks [1]. Viruses provide a particularly inspiring example. As first shown over 50 years ago for the tobacco mosaic virus [2], and later for a wide variety of other species, empty virus shells (capsids) can be made to reversibly self-assemble from individual protein subunits (capsomers) *in vitro*, simply by changing solution conditions such as the pH. Although this process resembles micellar self-assembly, there is an important difference: in contrast to the polydisperse distributions that characterise micelles, the closed virus capsids are monodisperse.

Understanding how such control and fidelity could be achieved with synthetically produced sub-units is an important goal for nanofabrication. New experimental techniques to create self-assembling systems are being rapidly developed [1]. Recent examples include the formation of tetrahedra from DNA strands [3], and the synthesis of anisotropic “patchy” colloidal particles [4, 5, 6].

These experimental advances have also stimulated much theoretical work. Important recent studies include work by Zhang and Glotzer who created anisotropic model particles by rigidly connecting spheres with different attractive potentials, and showed that these can form a rich variety of small cluster shapes and extended structures [7, 8]. Hagan and Chandler achieved the reversible self-assembly of large 60-particle virus models by using as their basic “capsomer” units spherical particles with directional anisotropic interactions that are chosen to be complementary in order to help guide the particles into the right local relative orientations [9]. This feature may easily be realised in protein-protein interactions but may be more difficult to implement in synthetic systems. Similarly, Van Workum and Douglas also found that virus-like assemblies (not necessarily monodisperse) formed from particles made up of three dipolar Stockmayer particles connected together to form triangles [10].

The authors above observed a diverse array of kinetic behaviour, including seeded nucleation [10], kinetic traps [9] and finite-size analogs to first or second order phase transitions [7].

In this paper we describe a set of minimal models, single spheres with anisotropic “patchy” interactions, that exhibit reversible self-assembly into monodisperse cluster phases. Choosing such simple systems facilitates the systematic exploration of parameter space to uncover the optimal design rules for self-assembly, and helps untangle the role of thermodynamic and kinetic factors.

Our model consists of spherical particles with a number of patches whose geometry is specified by a set of patch vectors. The repulsion is based on the isotropic Lennard-Jones potential

$$V_{\text{LJ}}(r) = 4\epsilon \left[\left(\frac{\sigma_{\text{LJ}}}{r} \right)^{12} - \left(\frac{\sigma_{\text{LJ}}}{r} \right)^6 \right], \quad (1)$$

but the attraction is modulated by an orientationally dependent term, V_{ang} . Thus, the complete potential is

$$V_{ij}(\mathbf{r}_{ij}, \mathbf{\Omega}_i, \mathbf{\Omega}_j) = \begin{cases} V_{\text{LJ}}(r_{ij}) & r < \sigma_{\text{LJ}} \\ V_{\text{LJ}}(r_{ij}) V_{\text{ang}}(\hat{\mathbf{r}}_{ij}, \mathbf{\Omega}_i, \mathbf{\Omega}_j) & r \geq \sigma_{\text{LJ}}, \end{cases} \quad (2)$$

where $\mathbf{\Omega}_i$ is the orientation of particle i . V_{ang} has the form:

$$V_{\text{ang}}(\hat{\mathbf{r}}_{ij}, \mathbf{\Omega}_i, \mathbf{\Omega}_j) = G_{ij}(\hat{\mathbf{r}}_{ij}, \mathbf{\Omega}_i) G_{ji}(\hat{\mathbf{r}}_{ji}, \mathbf{\Omega}_j) \quad (3)$$

$$G_{ij}(\hat{\mathbf{r}}_{ij}, \mathbf{\Omega}_i) = \exp\left(-\frac{\theta_{k_{\text{min}}ij}^2}{2\sigma^2}\right) \quad (4)$$

where σ is the standard deviation of the Gaussian, θ_{kij} is the angle between patch vector k on particle i and the interparticle vector \mathbf{r}_{ij} , and k_{min} is the patch that minimizes the magnitude of this angle. Hence, only the patches on each particle that are closest to the interparticle axis interact with each other.

In order to design these particles so that they self-assemble into monodisperse clusters with a particular

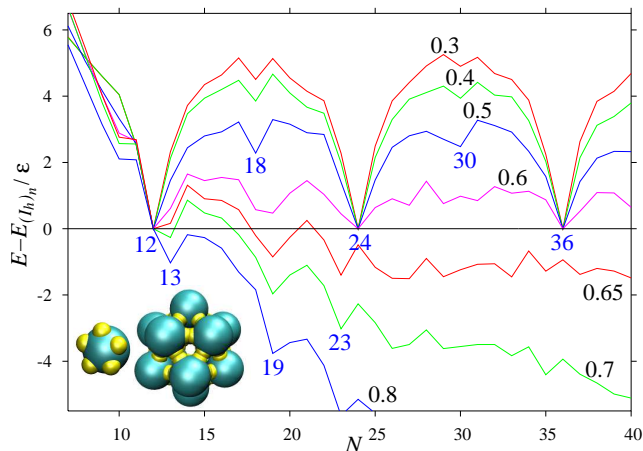


FIG. 1: (Colour Online) The size dependence of the energy of the global minimum for different values of σ . Each line is labelled by the value of σ (measured in radians), with particularly stable cluster sizes also labelled. The energy zero is a fit to the energies of the assemblies of complete icosahedra possible at $N=12, 24, 36$ and 48 at the appropriate value of σ . Hence, negative values indicate that it will never be energetically favourable for the system to form monodisperse icosahedra. In the bottom lefthand corner a single particle, and the 12-particle hollow icosahedron are illustrated.

target structure, the natural choice for the patch positions is to point them directly at the neighbouring particles in the target structure. The only parameter that remains to be optimized is then the patch width σ .

A minimal requirement for self-assembly is that the system of monodisperse clusters is energetically most stable. This is illustrated in Fig. 1 for 5-patch particles that are designed to stabilize the 12-particle hollow icosahedron. Global optimization (performed using the basin-hopping algorithm [11]) shows that for wider patches the global minima correspond to single compact clusters, but that for sufficiently narrow patches ($\sigma = 0.6$ and less) the most stable sizes occur at $N=12, 24, 36, \dots$, and do indeed correspond to packings of 1, 2, 3, \dots discrete icosahedra, as desired. The energy landscapes for such magic number clusters are likely to have a single-funnel topography [12].

To further investigate the self-assembly behaviour of our system, we performed Monte Carlo (MC) simulations in the canonical ensemble. By only using local displacements and rotations of the particles, the MC can be used as an approximate model of the dynamics. For computational efficiency, we truncate and shift the potential at $r = 3\sigma_{LJ}$. Fig. 2 illustrates a trajectory, and shows that, given the right conditions, the patchy particles are able to reversibly assemble into a monodisperse set of hollow icosahedral clusters.

The simplicity of our model allows us to map out in detail the assembly behaviour, thus enabling the optimal patch width and temperature to be identified. Fig. 3 summarizes results from 480 simulations at different com-

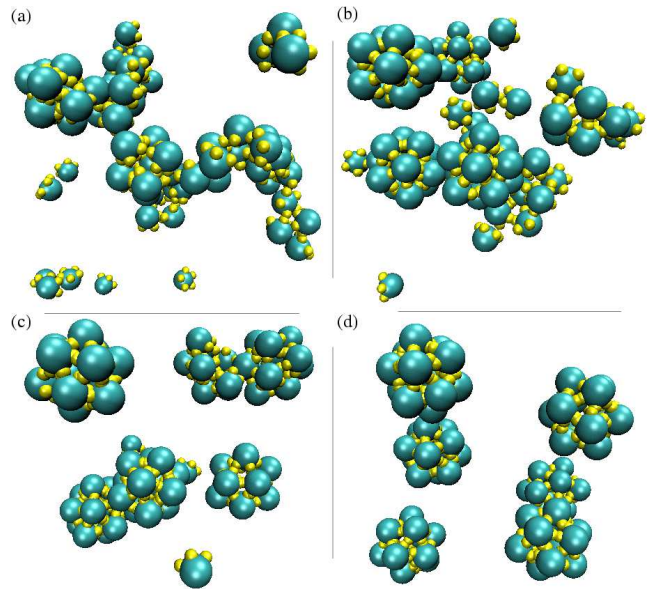


FIG. 2: (Colour Online) Snapshots of a system of 72 particles assembling into six complete icosahedra at $\sigma = 0.45$ and $T = 0.14 \epsilon k_B^{-1}$ after (a) 3000, (b) 8000, (c) 60 000 and (d) 250 000 MC cycles.

binations of σ and T , where each simulation was started from a disordered configuration generated at high temperature. Although this plot is for a particular density and after a certain number of MC moves, the generic features are not sensitive to these parameters.

The key feature of Fig. 3 is that there is a limited range in the space of patch width and temperature where self-assembly occurs efficiently. The maximum yield of 88% occurs at $\sigma = 0.45$ and $T = 0.14 \epsilon k_B^{-1}$ (for longer simulations we have observed yields up to 98%). To understand the assembly kinetics summarized in Fig. 3, we first examine the effect of temperature at the optimal σ . There is a clear maximum in the number of icosahedra formed, with the number dropping to zero at high and low temperature. The upper limit is thermodynamic because at high temperatures the stable phase of the system is a gas of monomers. The lower limit is kinetic and arises because at low temperatures the system does not have enough thermal energy to escape from incorrect arrangements of the particles, and so large low-density kinetic aggregates grow. These two limits are clearly visible from the mean cluster size plotted in Fig. 3(b).

Having such a temperature window where ordering can occur is common. For example, in the protein folding community it has been argued that increasing the ratio T_f/T_g (T_f is the ‘folding’ temperature at which the native state becomes most stable and T_g is the ‘glass’ transition temperature at which the dynamics becomes too slow for folding to occur) enhances the ability of a protein to fold [13]. Similarly, here we find that the optimal value of σ occurs roughly where there is the largest

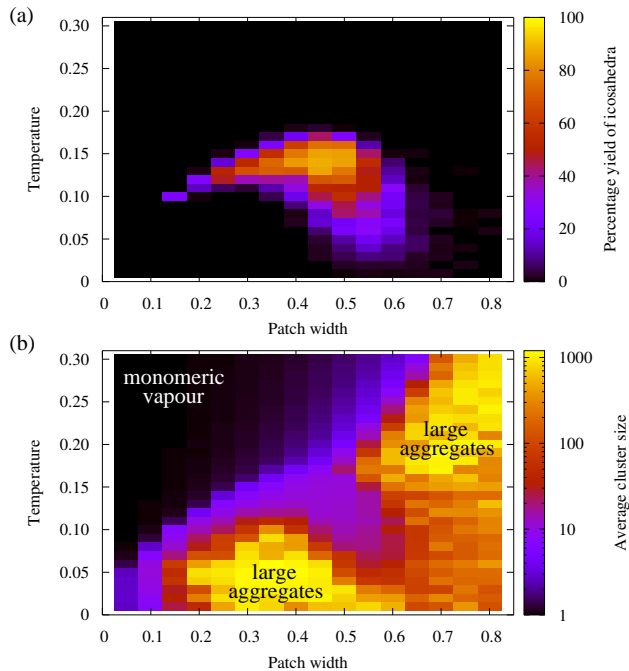


FIG. 3: (Colour Online) (a) The number of icosahedra formed and (b) the mean cluster size (averaged over particles) after 80 000 MC cycles as a function of the patch width σ (measured in radians) and the temperature for 1200 particles at a number density of $0.15 \sigma_{LJ}^{-3}$.

difference between T_{clust} , the temperature at which the clusters become thermodynamically most stable, and T_g , where the clustering is kinetically hindered.

The effect of reducing σ from its optimal value is to narrow the temperature window over which icosahedra form. Firstly, T_{clust} decreases as the patches become narrower, because the vibrational entropy of the icosahedral clusters decreases. Secondly, the potential becomes “stickier” as the patches narrow, and so the ‘glass transition’ temperature at which the particles becomes trapped in large non-equilibrium aggregates increases. Consequently, for $\sigma \leq 0.1$ icosahedra are virtually never seen.

Fig. 1 shows that beyond a certain σ , the icosahedra are no longer the most stable particle configuration. This is mirrored in Fig. 3(b) by the large disordered clusters, a liquid phase, that form for larger σ . Moreover, the interaction between the clustering transition and the liquid phase is particularly intriguing. For example, as the temperature is lowered for $\sigma \approx 0.55$, the system first condenses from a monomeric gas to a bulk liquid-like phase. However, at lower temperature it forms a gas again, but now made up of weakly interacting icosahedral clusters. This reentrant lower liquid-to-vapour transition is driven by the lower energy of the clusters, which overcomes the higher entropy of the liquid. Preliminary parallel tempering simulations have confirmed this unusual scenario.

Further information about the mechanisms of self-assembly can be gleaned from Fig. 4 which shows how

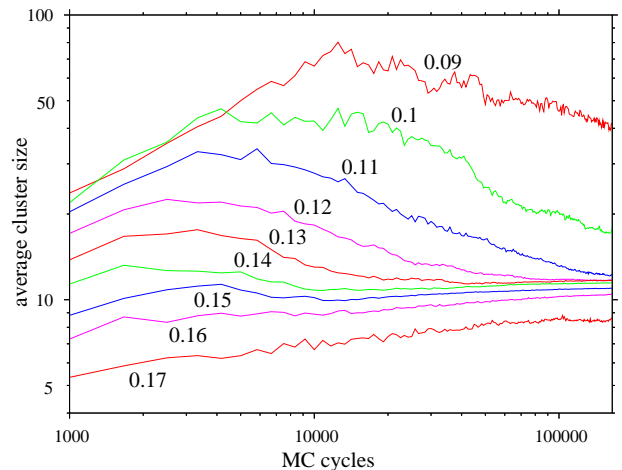


FIG. 4: (Colour Online) The mean cluster size as a function of number of MC cycles at $\sigma = 0.45$ at different temperatures (as labelled) for a system of 1200 particles at a number density of $0.15 \sigma_{LJ}^{-3}$. Each line is an average over 10 simulations.

the average cluster size evolves with MC time for different temperatures at the optimal patch width. One striking feature is that for $T \gtrsim 0.14 \epsilon k^{-1}$ the average cluster size goes through a maximum before decreasing towards twelve. The pathway to cluster formation is through larger disordered clusters, which then “bud off” icosahedra, rather than through the growth of icosahedra from smaller units. The height of this maximum increases with decreasing temperature because the rate of growth increases compared to the rate at which icosahedra are annealed out. The self-assembly of icosahedra is therefore facilitated by the formation of a metastable intermediate phase, and the liquid phase, which we previously noted is stable at larger σ , plays an important role, even when it has disappeared from the equilibrium phase diagram. This system therefore provides an example of Ostwald’s step rule [14] where nucleation initially leads to a metastable phase. For example, protein crystallization can be enhanced by the formation of a metastable protein-rich phase from which the crystal can more easily nucleate [15, 16].

The above mechanism of self-assembly is very different from that so far observed in experimental [17, 18, 19] and theoretical (both kinetic models [19, 20] and direct simulations [9]) work on viruses, where direct nucleation of the virus capsid is the norm. We see a crossover to this type of mechanism at higher temperature and lower patch width, the latter because the system is then further away from the range of parameters where there is a stable liquid phase [21].

The same approach that we have used to design particles that form monodisperse icosahedra can also be applied to other target structures. For example, we have been able to assemble tetrahedra, octahedra and cubes from particles with the right number of correctly-oriented

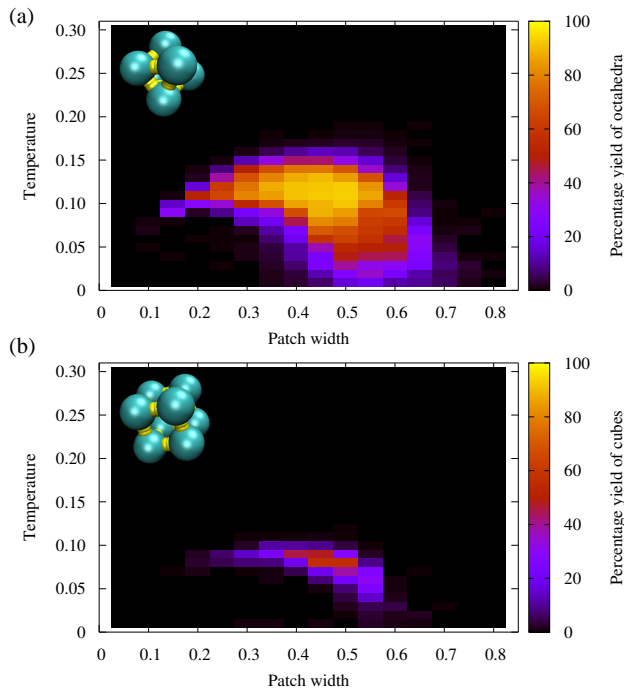


FIG. 5: (Colour Online) The number of (a) octahedra and (b) cubes (expressed as a percentage of the maximum possible) formed after 80 000 MC cycles as a function of the patch width σ and the temperature for 1200 particles at a number density of $0.15 \sigma_{LJ}^{-3}$.

patches. We were also able to assemble icosahedra from particles by creating a single ring patch with the right cone angle. This was inspired by the work of Ref. [7], although we use a single uniform ring, not a composite ring with two types of interactions.

These simulations confirmed that the basic physics of self-assembly is very similar to that for the icosahedra, as illustrated in Fig. 5 for octahedra and cubes. These plots have the same characteristic shape as Fig. 3(a). Note that the temperature window over which the cubes form is much narrower than for the other shapes. This appears to be due to a lowering of T_{clust} , in part because there are only three patches per particle stabilizing the cube. Just as for the icosahedra, we also observe a multiplicity of dynamic pathways to self-assembly.

From these results we can learn something about the general principles required when designing objects to self-assemble. The optimal value of σ represents a compromise between the energetic and kinetic requirements for self-assembly. As σ is decreased, the energy gap between the target structure and other possible competing structures increases. By contrast, kinetic accessibility improves as σ increases, because the system is more easily able to escape from incorrect configurations. The lesson is that the interactions need to be specific enough to sufficiently favour the target structure, but that over-specifying them can inhibit the dynamics of assembly.

Another lesson is that the dynamic pathways to self-assembly can be complex and non-intuitive. We found, for example, that, besides the better known nucleation pathways, clusters could also form through disordered intermediates, a process also observed for bulk phases and explained by the Ostwald step rule [14].

Our study focussed on simple models in order to be able to explore the design space in detail. Although these patchy spheres are clearly much more basic than the units involved in monodisperse self-assembly in biological systems, the comprehensive understanding that this simplicity allows us to achieve should provide useful insights into the biological examples. Furthermore, this feature may be an advantage when considering the design of synthetic self-assembling building blocks.

The authors are grateful to the Engineering and Physical Sciences Research Council, the Royal Society, the Ramón Areces Foundation and Churchill College, Cambridge for financial support.

* Authors for correspondence

- [1] G. M. Whitesides and B. Grzybowski, *Science* **295**, 2418 (2002).
- [2] H. Fraenkel-Conrat and R. C. Williams, *Proc. Natl. Acad. Sci. USA* **41**, 690 (1955).
- [3] R. P. Goodman, I. A. T. Schaap, C. F. Tardin, C. M. Erben, R. M. Berry, C. F. Schmidt, and A. J. Turberfield, *Nature* **310**, 1661 (2005).
- [4] Y.-S. Cho, G.-R. Yi, J.-M. Lim, S.-H. Kim, V. N. Manoharan, D. J. Pine, and S.-M. Yang, *J. Am. Chem. Soc.* **127**, 15968 (2005).
- [5] K.-H. Roh, D. C. Martin, and J. Lahann, *Nature Materials* **4**, 759 (2005).
- [6] A. M. Jackson, J. W. Myerson, and F. Stellacci, *Nature Materials* **3**, 330 (2004).
- [7] Z. Zhang and S. C. Glotzer, *Nano Lett.* **4**, 1407 (2004).
- [8] S. C. Glotzer, *Science* **306**, 419 (2004).
- [9] M. F. Hagan and D. Chandler, *Biophys. J.* **91**, 42 (2006).
- [10] K. van Workum and J. F. Douglas, *Phys. Rev. E* **73**, 031502 (2006).
- [11] D. J. Wales and J. P. K. Doye, *J. Phys. Chem. A* **101**, 5111 (1997).
- [12] D. J. Wales, *Phil. Trans. R. Soc. A* **363**, 357 (2005).
- [13] J. D. Bryngelson, J. N. Onuchic, N. D. Socci, and P. G. Wolynes, *Proteins* **21**, 167 (1995).
- [14] W. Ostwald, *Z. Phys. Chem.* **22**, 289 (1897).
- [15] P. R. ten Wolde and D. Frenkel, *Science* **277**, 1975 (1997).
- [16] D. Vivarès, E. W. Kaler, and A. M. Lenhoff, *Acta. Cryst. D* **61**, 819 (2005).
- [17] G. L. Casini, D. Graham, D. Heine, R. L. Garcea, and D. T. Wu, *Virology* **325**, 320 (2004).
- [18] K. N. Parent, S. M. Doyle, E. Anderson, and C. M. Teschke, *Virology* **340**, 33 (2005).
- [19] A. Zlotnick and S. J. Stray, *Trends Biotechnol.* **21**, 536 (2003).
- [20] D. Endres and A. Zlotnick, *Biophys. J.* **83**, 1217 (2002).
- [21] Z. Tavassoli and R. P. Sear, *J. Chem. Phys.* **116**, 5066 (2002).